DETECTION OPTIMIZATION FOR THE DCT-DOMAIN IMAGE WATERMARKING SYSTEM

Slobodan Djukanović and Igor Djurović

University of Montenegro/Electrical Engineering Department
Cetinjska 2, 81 000, Podgorica, Montenegro
phone: + (382) 20 245 839, fax: + (382) 20 245 873, email: {slobdj,igordj}@ac.me

ABSTRACT

This paper proposes a detection optimization for the DCT-domain image watermarking system developed by Barni *et al*. The visual masking introduced in this scheme causes performance deterioration in the watermark detection. We therefore modify the searched watermark, by using linear algebra methods, taking into account the influence of the visual masking on the watermark detection. The optimized detection outperforms the standard one for both non-attacked images and images subjected to a number of standard attacks. In addition, it allows detection of very weak watermarks. The optimization process requires a few percents of the original DCT coefficients.

1. INTRODUCTION

Digital watermarking has tremendous importance nowadays since for the first time in human history perfect replication of intellectual works is possible. The cornerstone in the area was the famous paper [1], in which a class of very powerful spread spectrum watermarking systems is introduced. Numerous alternative approaches have been developed, mainly based on correlation techniques similar to that proposed in [1]. These techniques are applied in time and space domain [2, 3], spectral domain [4]–[7], or combined space-frequency domains [8]. However, watermarking challenges have been constantly growing. For example, many of proposed sophisticated attacks are able to remove embedded watermarks without significant distortion to the multimedia data. Moreover, various applications put difficult requirements for the watermarking techniques. For example, watermarking in medical applications should be as low as possible in order to avoid disturbances to sensitive information that medical images contain [9].

In this paper, we propose a detection optimization method for the watermarking technique proposed in [7], where the watermark invisibility is improved by the visual masking. This masking, however, deteriorates the watermark detection. We propose a way to optimize the detection considering the influence of the visual masking on the performance of detector. The term *optimization* will refer to a modification of watermark the detector searches for in order to maximize the distance between the probability density functions (PDFs) of the correlator output when the searched watermark and the embedded one do not coincide and when they do coincide. The distance maximization will be performed by using linear algebra methods, and detector characterized by maximal distance between these two PDFs will be referred to as an *optimal watermark detector*, whereas detector with no optimization performed will be referred to as a *standard watermark detector*.

An overview of the DCT-domain watermarking technique is given in Section 2. In Section 3, we define the detection optimization method, whose performance is evaluated in Section 4. Conclusions are drawn in Section 5.

2. THE DCT-DOMAIN WATERMARKING SYSTEM

The DCT of an $N \times N$ greyscale image $\mathbf{I}$, $\mathbf{D}_I$, and its inverse are defined as follows:

$$D_I(i,j) = \mathrm{DCT}(\mathbf{I}) = C(i,j) \sum_{m,n=0}^{N-1} I(m,n)\, q_{mi} q_{nj} \quad (1)$$

$$I(m,n) = \mathrm{IDCT}(\mathbf{D}_I) = \sum_{i,j=0}^{N-1} C(i,j)\, D_I(i,j)\, q_{mi} q_{nj}, \quad (2)$$

where

$$q_{ij} = \cos \frac{\pi (2i+1) j}{2N}, \quad (3)$$

and $\mathbf{C}$ is the $N \times N$ matrix with

$$C(i,j) = \begin{cases} 1/N & i = 0 \text{ and } j = 0 \\ 2/N & i > 0 \text{ and } j > 0 \\ \sqrt{2}/N & \text{otherwise.} \end{cases} \quad (4)$$

In [7], watermark $\mathbf{W} = \{w_1, w_2, ..., w_L\}$ to be embedded is an L samples long pseudo-random sequence, where w_i, $i = 1, 2, ..., L$, are i.i.d. Gaussian variables with zero mean and unity variance. The watermark is superimposed on a fixed set of coefficients of $\mathrm{DCT}(\mathbf{I})$. The set is obtained by reordering $\mathrm{DCT}(\mathbf{I})$ into the zigzag scan and taking the coefficients from the $(P+1)$th to the $(P+L)$th position, thus forming a vector $\mathbf{D} = \{d_{P+1}, d_{P+2}, ..., d_{P+L}\}$. The first P coefficients are skipped so that the perceptual invisibility is attained. The watermark $\mathbf{W}$ is embedded into the image $\mathbf{I}$ by replacing DCT coefficients d_{P+i} with

$$d'_{P+i} = d_{P+i} + \alpha w_i |d_{P+i}|, \quad i = 1, 2, ..., L, \quad (5)$$

where α is a scaling parameter. The watermarked image $\mathbf{I}'$ is obtained by calculating the IDCT of the DCT with the embedded watermark.

In the watermark detection, we calculate the correlation

$$z = \frac{1}{L} \sum_{i=1}^{L} d^*_{P+i} \overline{w}_i, \quad (6)$$

where $\overline{\mathbf{W}} = \{\overline{w}_1, \overline{w}_2, ..., \overline{w}_L\}$ is the searched watermark and $\mathbf{D}^* = \{d^*_{P+1}, d^*_{P+2}, ..., d^*_{P+L}\}$ is the vector of the DCT coefficients of possibly corrupted image $\mathbf{I}^*$. The correlation z can be used for deciding whether a given mark is present by comparing z to a predefined threshold, or as the basis of distinction between a set of known marks by calculating z for all marks and declaring a mark with the largest z to be the one present in the image [7].

 ISSN 2076-1465

The mean and variance of z satisfy [7]

$$\mu_z = \begin{cases} 0 & \text{if } \overline{\mathbf{W}} \neq \mathbf{W} \text{ or no mark is present} \\ \alpha\mu_{|d|} & \text{if } \overline{\mathbf{W}} = \mathbf{W} \end{cases} \quad (7)$$

$$\sigma_z^2 \approx \sigma_d^2/L, \quad (8)$$

where $\mu_{|d|}=E[|d_{P+i}|]$ and $\sigma_d^2=\mathrm{Var}[d_{P+i}]$. $E[\cdot]$ and $\mathrm{Var}[\cdot]$ respectively denote the expectation and variance operators. Approximation (8) is valid for $\alpha^2 \ll 1$. The detector therefore yields two Gaussian random variables, z_1 and z_2, with the same variance σ_z^2 and means 0 and $\alpha\mu_{|d|}$, respectively.

The distance between the PDF curves of z_1 and z_2,

$$k_z = \mu_z/\sigma_z, \quad (9)$$

provides the measure of goodness of the watermark detector. Any increase in k_z can significantly reduce the error probability in the watermark detection. The error probability can be approximated as $P_e = 0.5\mathrm{erfc}(\mu_{z_2}/(2\sqrt{2}\sigma_{z_2}))$, where $\mathrm{erfc}(x)$ is the complementary error function [7]. For instance, an increase of μ_{z_2}/σ_{z_2} from 3 to 4 decreases P_e from 6.68% to 2.28%.

The watermark invisibility can be additionally improved by visually masking the watermarked image $\mathbf{I}'$ given by

$$I''(i,j) = [1-R(i,j)]\,I(i,j) + R(i,j)\,I'(i,j), \quad (10)$$

where $R(i,j)$ equals the normalized variance calculated within the $H \times H$ block centered at the (i,j) pixel of $\mathbf{I}$ [7]. Spatial regions with high variance give $R(i,j) \approx 1$ and therefore $I''(i,j) \approx I'(i,j)$, whereas uniform regions give $R(i,j) \approx 0$ and $I''(i,j) \approx I(i,j)$.

A downside to the visual masking is the influence of the matrix $\mathbf{R}$ on the watermarked DCT coefficients, and, in turn, on the watermark detection. Optimization of the watermark detection, taking into account the influence of $\mathbf{R}$ on detector's performance, is the subject of the rest of the paper.

3. WATERMARK DETECTION OPTIMIZATION

3.1 Watermarking and visual masking in matrix form

According to (5), the watermark embedding is

$$\begin{aligned} D_I'(i,j) &= D_I(i,j) + \alpha W(i,j)\,B(i,j)\,|D_I(i,j)| \\ &= D_I(i,j) + X(i,j). \end{aligned} \quad (11)$$

In order to make (11) equivalent to the embedding form (5), an $N \times N$ matrix $\mathbf{B}$ is introduced to ensure that the watermark is embedded only into the proper DCT coefficients. The matrix $\mathbf{B}$ is therefore defined as

$$B(i,j) = \begin{cases} 1 & \text{watermark is embedded into } D_I(i,j) \\ 0 & \text{otherwise.} \end{cases} \quad (12)$$

The $N \times N$ watermark matrix $\mathbf{W}$ satisfies

$$E[W(i,j)] = 0 \quad (13)$$

$$E[W(i,j)\,W(k,l)] = \sigma_W^2\,\delta(i-k, j-l) \quad (14)$$

$$E[W(i,j)\,D_I(i,j)] = 0, \quad (15)$$

where $\delta(m,n)$ is the 2D Dirac delta function. The $N \times N$ matrix $\mathbf{X}$ is introduced to shorten the notation and the value of $X(i,j)$ is clear from (11). Now the watermark embedding in matrix form reads

$$\mathbf{D}_I' = \mathbf{D}_I + \alpha\mathbf{W} \bullet \mathbf{B} \bullet |\mathbf{D}_I| = \mathbf{D}_I + \mathbf{X}, \quad (16)$$

where $\bullet$ is the Hadamard (entrywise) product operator. The watermarked image $\mathbf{I}'$ is obtained as

$$I'(m,n) = \mathrm{IDCT}\left(\mathbf{D}_I'\right) = I(m,n) + X'(m,n), \quad (17)$$

where $X'(m,n) = \mathrm{IDCT}(\mathbf{X})$.

The visual masking (10) in matrix form is given as

$$\mathbf{I}'' = (\mathbf{1}-\mathbf{R}) \bullet \mathbf{I} + \mathbf{R} \bullet \mathbf{I}' = \mathbf{I} + \mathbf{R} \bullet \mathbf{X}', \quad (18)$$

where $\mathbf{1}$ represents the $N \times N$ all-ones matrix.

The correlation z, as defined by (6), equals

$$z = \frac{1}{L}\sum_{m,n=0}^{N-1} D_{I''}(m,n)\,\overline{W}(m,n)\,B(m,n), \quad (19)$$

where

$$D_{I''}(m,n) = \mathrm{DCT}\left(\mathbf{I}''\right) = D_I(m,n) + D_{RX}(m,n) \quad (20)$$

and

$$\begin{aligned} D_{RX}(m,n) &= \mathrm{DCT}\left(\mathbf{R} \bullet \mathbf{X}'\right) \\ &= C(m,n)\textstyle\sum_{i,j=0}^{N-1} R(i,j)\,X'(i,j)\,q_{im}q_{jn} \\ &= \alpha C(m,n)\textstyle\sum_{i,j=0}^{N-1} R(i,j)\,q_{im}q_{jn} \\ &\times \textstyle\sum_{u,v=0}^{N-1} C(u,v)\,W(u,v)\,B(u,v)\,|D_I(u,v)|\,q_{iu}q_{jv}. \end{aligned} \quad (21)$$

The matrix $\mathbf{B}$ in (19) enforces the correlation to be limited only to the DCT coefficients the watermark is originally embedded into.

3.2 Detection optimization - A whole watermark at once

The distance k_z, according to (9), depends on $E[z]$ when $\overline{\mathbf{W}} = \mathbf{W}$; the following analysis therefore assumes $\overline{\mathbf{W}} = \mathbf{W}$.

The detection optimization will be done by multiplying $\overline{\mathbf{W}}$, prior to the detection, by an $N \times N$ matrix $\mathbf{M}$, i.e.

$$\mathbf{W}_M = \mathbf{M}\,\overline{\mathbf{W}} = \mathbf{M}\,\mathbf{W}, \quad (22)$$

which, in turn, yields

$$z = \frac{1}{L}\sum_{m,n,k=0}^{N-1} D_{I''}(m,n)\,M(m,k)\,W(k,n)\,B(m,n). \quad (23)$$

In this paper, instead of k_z its squared value

$$K_z = k_z^2 = E^2[z]/\mathrm{Var}[z] \quad (24)$$

will be maximized. The optimization problem therefore reduces to finding a matrix $\mathbf{M}$ that maximizes K_z.

Let us start with $E[z]$. According to (23), (20) and (15), we get

$$E[z] = \textstyle\sum_{m,n,k} E[D_{RX}(m,n)\,W(k,n)]\,M(m,k)\,B(m,n), \quad (25)$$

where m, n and k run from 0 to $N-1$. The scaling factor $\frac{1}{L}$ has been dropped in (25) since $\frac{1}{L^2}$ appears in both the numerator and denominator of K_z. Now, by substituting (21) into (25), we have

$$\begin{aligned} E[z] &= \alpha\sigma_W^2 \textstyle\sum_{m,n,k} M(m,k)\,B(m,n)\,C(m,n)\,C(k,n) \\ &\times B(k,n)\,|D_I(k,n)| \textstyle\sum_{i,j} R(i,j)\,q_{ik}q_{im}q_{jn}^2 \\ &= \alpha\sigma_W^2 \textstyle\sum_{m,k} M(m,k) \sum_{i,j} R(i,j)\,q_{ik}q_{im} \\ &\times \textstyle\sum_n C_B(m,n)\,C_B(k,n)\,|D_I(k,n)|\,q_{jn}^2, \end{aligned} \quad (26)$$

where

$$\mathbf{C}_B = \mathbf{C} \bullet \mathbf{B} \tag{27}$$

and i and j also run from 0 to $N-1$. By introducing the $N \times N$ matrix $\mathbf{\Theta}$ with entries

$$\begin{aligned}\Theta(k,m) =& \alpha\sigma_W^2 \sum_{i,j} R(i,j)\, q_{ik} q_{im} \\ & \times \sum_n C_B(k,n)\, C_B(m,n)\, |D_I(k,n)|\, q_{jn}^2,\end{aligned} \tag{28}$$

$E[z]$ reduces to

$$E[z] = \sum_{m,k} M(m,k)\, \Theta(k,m). \tag{29}$$

Define

$$\mathbf{M}_1^T = [\mathbf{m}_1\ \mathbf{m}_2\ \cdots\ \mathbf{m}_N]_{1\times N^2} \tag{30}$$

$$\mathbf{\Theta}_1^T = \left[\theta_1^T\ \theta_2^T\ \cdots\ \theta_N^T\right]_{1\times N^2}, \tag{31}$$

where $(\cdot)^T$ represents the transpose operator, $\mathbf{m}_i$ is the $1 \times N$ vector (ith row of the matrix $\mathbf{M}$) and θ_i is the $N \times 1$ vector (ith column of the matrix $\mathbf{\Theta}$) and $i = 1, 2, ..., N$. Now it holds

$$E[z] = \mathbf{M}_1^T \mathbf{\Theta}_1. \tag{32}$$

As for the variance Var$[z]$, we will give only the final matrix form due to the limited paper length[1]. It is

$$\mathrm{Var}[z] = \mathbf{M}_1^T (\mathbf{\Omega}_1 + \mathbf{\Phi}_1 + \mathbf{\Lambda}_1)\, \mathbf{M}_1, \tag{33}$$

where the $N^2 \times N^2$ matrices $\mathbf{\Omega}_1$, $\mathbf{\Phi}_1$ and $\mathbf{\Lambda}_1$ are defined below (relations (34), (37) and (40), respectively),

$$\mathbf{\Omega}_1 = \begin{bmatrix} \omega_{11} & \omega_{12} & \cdots & \omega_{1N} \\ \omega_{21} & \omega_{22} & \cdots & \omega_{2N} \\ \vdots & \vdots & \ddots & \vdots \\ \omega_{N1} & \omega_{N2} & \cdots & \omega_{NN} \end{bmatrix}, \tag{34}$$

where $\omega_{m_1 m_2}$ is the $N \times N$ matrix defined by

$$\omega_{m_1 m_2} = \Omega(m_1, m_2)\, \mathbf{I}, \tag{35}$$

and $\mathbf{I}$ is the $N \times N$ identity matrix and

$$\begin{aligned}\Omega(m_1,m_2) =& \alpha^2\sigma_W^4 \sum_{i_1,i_2,j_1,j_2} R(i_1,j_1) R(i_2,j_2) \\ & \times q_{i_1 m_1} q_{i_2 m_2} \sum_{n_1} C_B(m_1,n_1)\, C_B(m_2,n_1)\, q_{j_1 n_1} q_{j_2 n_1} \\ & \times \sum_{u,v} C_B^2(u,v)\, D_I^2(u,v)\, q_{i_1 u} q_{i_2 u} q_{j_1 v} q_{j_2 v},\end{aligned} \tag{36}$$

$$\mathbf{\Phi}_1 = [\phi_{11} \cdots \phi_{1N}\ \phi_{21} \cdots \phi_{2N} \cdots \phi_{N1} \cdots \phi_{NN}], \tag{37}$$

where ϕ_{ij} is the $N^2 \times 1$ vector defined as

$$\begin{aligned}\phi_{ij} = [&\Phi(1,1,i,j), \cdots, \Phi(1,N,i,j), \Phi(2,1,i,j), \cdots, \\ &\Phi(2,N,i,j), \cdots, \Phi(N,1,i,j), \cdots, \Phi(N,N,i,j)]^T\end{aligned} \tag{38}$$

and

$$\begin{aligned}\Phi(m_1,k_1,m_2,k_2) =& \alpha^2\sigma_W^4 \\ & \times \sum_{i_1,i_2,j_1,j_2} R(i_1,j_1) R(i_2,j_2)\, q_{i_1 m_1} q_{i_2 m_2} q_{i_1 k_2} q_{i_2 k_1} \\ & \times \sum_{n_1} C_B(m_1,n_1)\, C_B(k_1,n_1)\, |D_I(k_1,n_1)|\, q_{j_1 n_1} q_{j_2 n_1} \\ & \times \sum_{n_2} C_B(m_2,n_2)\, C_B(k_2,n_2)\, |D_I(k_2,n_2)|\, q_{j_1 n_2} q_{j_2 n_2}.\end{aligned} \tag{39}$$

[1] Full derivation is available at request.

Finally

$$\mathbf{\Lambda}_1 = \begin{bmatrix} \lambda_{11} & \lambda_{12} & \cdots & \lambda_{1N} \\ \lambda_{21} & \lambda_{22} & \cdots & \lambda_{2N} \\ \vdots & \vdots & \ddots & \vdots \\ \lambda_{N1} & \lambda_{N2} & \cdots & \lambda_{NN} \end{bmatrix}, \tag{40}$$

where λ_{ij} is the $N \times N$ matrix defined by

$$\lambda_{ij} = \Lambda(i,j)\, \mathbf{I}$$

and

$$\Lambda(i,j) = \sigma_W^2 \sum_n B(i,n)\, B(j,n)\, D_I(i,n)\, D_I(j,n). \tag{41}$$

In (36), (39) and (41), all the summation variables run from 0 to $N-1$.

The ratio K_z can be finally expressed as

$$K_z = \frac{\mathbf{M}_1^T \mathbf{\Theta}_1 \mathbf{\Theta}_1^T \mathbf{M}_1}{\mathbf{M}_1^T (\mathbf{\Omega}_1 + \mathbf{\Phi}_1 + \mathbf{\Lambda}_1)\, \mathbf{M}_1} = \frac{\mathbf{M}_1^T \mathbf{Z} \mathbf{M}_1}{\mathbf{M}_1^T \mathbf{Y} \mathbf{M}_1}, \tag{42}$$

where the $N^2 \times N^2$ matrices $\mathbf{Z}$ and $\mathbf{Y}$ are clear from (42). The final form of K_z may be viewed as the Rayleigh quotient [10]. The matrices $\mathbf{\Omega}_1$, $\mathbf{\Phi}_1$ and $\mathbf{\Lambda}_1$ are symmetric implying that $\mathbf{Y}$ and $\mathbf{Y}^{1/2}$ are also symmetric. We can therefore define the $N^2 \times 1$ vector $\hat{\mathbf{M}}_1 = \mathbf{Y}^{1/2} \mathbf{M}_1$ and express (42) as

$$K_z = \frac{\hat{\mathbf{M}}_1^T \left[(\mathbf{Y}^{-1/2})^T\, \mathbf{Z}\, \mathbf{Y}^{-1/2}\right] \hat{\mathbf{M}}_1}{\hat{\mathbf{M}}_1^T \hat{\mathbf{M}}_1}. \tag{43}$$

The Rayleigh quotient states that K_z reaches its maximum when $\hat{\mathbf{M}}_1$ is an eigenvector of the $N^2 \times N^2$ matrix $(\mathbf{Y}^{-1/2})^T\, \mathbf{Z}\, \mathbf{Y}^{-1/2}$ that corresponds to its largest eigenvalue. If we denote such a vector as $\hat{\mathbf{M}}_{1\max}$, the optimal detector is obtained by rearranging the $N^2 \times 1$ optimal vector

$$\mathbf{M}_{1\mathrm{opt}} = \mathbf{Y}^{-1/2}\, \hat{\mathbf{M}}_{1\max} \tag{44}$$

back into the $N \times N$ matrix $\mathbf{M}$ according to (30). The detector that implements the modification of the watermark $\mathbf{W}$ by such a matrix $\mathbf{M}$ will be referred to as the optimal detector, as opposed to the standard detector obtained for $\mathbf{M} = \mathbf{I}$.

The previous analysis is computationally acceptable only for smaller images. This is due to the fact that the introduced optimization requires the calculation of eigenvalues of an $N^2 \times N^2$ matrix, which for bigger N (e.g., $N = 512$) far exceeds the capacity of commercial computers nowadays. The proposed algorithm will be therefore modified in order to make the processing of bigger images possible.

3.3 Detection optimization - A block optimization

By dividing the matrices $\mathbf{D}_{I''}$, $\mathbf{W}$ and $\mathbf{B}$ into adjacent non-overlapping $N_1 \times N_1$ submatrices, the correlation (19) can be rewritten as the sum of partial correlations $z^{\gamma\rho}$, i.e.

$$z = \frac{1}{L} \sum_{\gamma,\rho=0}^{K-1} z^{\gamma\rho}, \tag{45}$$

where K is an integer satisfying $K = \frac{N}{N_1}$, and

$$z^{\gamma\rho} = \sum_{m,n=0}^{N_1-1} D_{I''}^{\gamma\rho}(m,n)\, W^{\gamma\rho}(m,n)\, B^{\gamma\rho}(m,n), \tag{46}$$

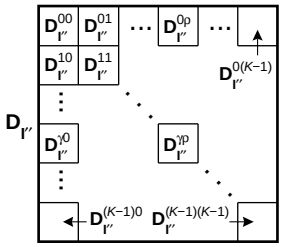

Figure 1: The $N \times N$ matrix $\mathbf{D}_{I''}$ is divided into the $N_1 \times N_1$ matrices $\mathbf{D}_{I''}^{\gamma\rho}$; γ and ρ run from 0 to $K-1$, and $K = \frac{N}{N_1}$.

where $\mathbf{D}_{I''}^{\gamma\rho}$, $\mathbf{W}^{\gamma\rho}$ and $\mathbf{B}^{\gamma\rho}$ are the $N_1 \times N_1$ submatrices of $\mathbf{D}_{I''}$, $\mathbf{W}$ and $\mathbf{B}$, respectively, defined by

$$\begin{aligned} D_{I''}^{\gamma\rho}(m,n) &= D_{I''}(m+\gamma N_1, n+\rho N_1) \\ W^{\gamma\rho}(m,n) &= W(m+\gamma N_1, n+\rho N_1) \\ B^{\gamma\rho}(m,n) &= B(m+\gamma N_1, n+\rho N_1), \end{aligned} \tag{47}$$

where m and n run from 0 to $N_1 - 1$. In Figure 1, $\mathbf{D}_{I''}$ is divided into the submatrices $\mathbf{D}_{I''}^{\gamma\rho}$.

Instead of the optimization of the whole correlation at once, the partial correlations $z^{\gamma\rho}$ will be now separately optimized by using the approach developed in the previous section. To this end, the matrix $\mathbf{W}^{\gamma\rho}$ is modified by an $N_1 \times N_1$ matrix $\mathbf{M}$, which will be determined to maximize the ratio

$$K_z^{\gamma\rho} = \left(k_z^{\gamma\rho}\right)^2 = E^2\left[z^{\gamma\rho}\right] / \mathrm{Var}\left[z^{\gamma\rho}\right]. \tag{48}$$

The optimization procedure is carried out for each $\gamma\rho$ block separately, excluding blocks with the all-zeros matrix $\mathbf{B}^{\gamma\rho}$. Since the final matrix form of $K_z^{\gamma\rho}$ is very similar to the one given by (42), we will omit it here.

3.4 Discussion

The matrices $\mathbf{\Theta}_1$, $\mathbf{\Omega}_1$, $\mathbf{\Phi}_1$ and $\mathbf{\Lambda}_1$ depend on $\mathrm{DCT}(\mathbf{I})$. It can be shown, however, that our analysis does not require all the DCT coefficients, but only those the watermark is embedded into. A closer look at these matrices reveals that they include the term of the form $C_B(k,n) D_I(k,n)$, which, due to (12) and (27), implies that coefficients $D_I(k,n)$ the watermark is not embedded into will not affect the value of K_z. For instance, in (28) we have $C_B(k,n)|D_I(k,n)|$, in (36) there is $C_B^2(u,v) D_I^2(u,v)$ etc.

The watermark is usually embedded into a few percents of the DCT coefficients. These coefficients should be submitted within the image header file and protected using some of the standard cryptographic techniques. A user can read the image file without any difficulties and only the copyright protection checking involves the submitted coefficients.

Future research activities will include the modification of the proposed method so that it uses statistical properties of the DCT coefficients instead of their original values.

4. EXPERIMENTAL RESULTS

We will start with the evaluation of performance of the proposed detector when the whole watermark is optimized at once, as presented in Section 3.2. The Baboon and Boat images with $N = 32$ are considered. This image size is of no practical significance; rather, it will be used only to verify the validity of the underlying method. Therefore, none of the attacks will be considered at this point. The embedded watermark has zero mean and $\sigma_W^2 = 1$; it is embedded starting from $P = 300$ and $L = 300$. The matrix $\mathbf{R}$ is calculated with $H = 9$, and the mean value of α, after weighting by $R(i,j)$ [7], is $\overline{\alpha} = 0.3$. In the watermark detection stage, 1000 watermarks are generated and the embedded one is at position 100. Normalized detector responses for the standard and optimal detectors are shown in Figure 2. For the numerical comparison of these two detectors, the variance of the normalized detector response, σ_{znor}^2, is calculated and shown on the corresponding plot, along with the distance k_z. The simulations were also carried out with other standard images (Lena, Stream and bridge, Peppers, Man) and similar results were obtained. The optimal detector outperforms the standard one, thus giving us the green light to test it on bigger images.

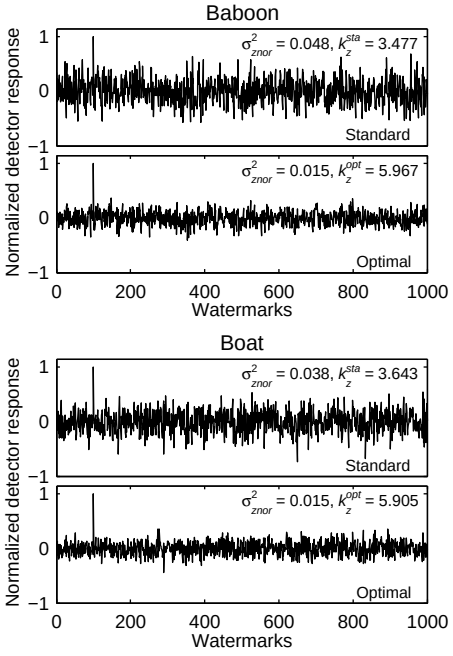

Figure 2: Normalized detector response for the standard and optimal detectors.

Consider now the same images with $N = 512$. The same form of watermark $\mathbf{W}$ is adopted, with $P = 2000$, $L = 8000$ and $\overline{\alpha} = 0.1$ (which corresponds to the peak signal-to-noise ratio (PSNR) of 39.70dB) and the matrix $\mathbf{R}$ is calculated with $H = 9$. We performed the detection optimization, with $N_1 = 8$, for the non-attacked images and for the images subjected to a number of attacks listed in Table 1. The variances σ_{znor}^2 of the normalized detector responses are shown in Table 1. The both detectors have successfully detected the embedded watermark. The optimal detector, however, outperforms the standard one in terms of σ_{znor}^2 for all the cases. The simulations were also performed with other standard images and similar results were obtained.

Finally, we considered the case when the watermark is very weak. The watermarking parameters are same as in the previous example. No attacks will be considered herein; rather, the possibility of the optimized detector to detect a

Table 1: Variance σ^2_{znor} of normalized detector responses

	Baboon		**Boat**	
	Stand.	Opt.	Stand.	Opt.
No attack	0.021	0.004	0.030	0.005
JPEG compression (0% smoothing and 10% quality)	0.022	0.007	0.040	0.010
Histogram equalization	0.029	0.008	0.023	0.016
Histogram stretching	0.025	0.004	0.025	0.005
Low pass filtering (filter 5×5)	0.029	0.010	0.025	0.017
Median filtering (filter 5×5)	0.030	0.008	0.032	0.007
Dithering	0.025	0.006	0.026	0.006
Resize from 512×512 to 256×256	0.026	0.016	0.034	0.016
AWGN with the variance of 900	0.025	0.016	0.034	0.014
Multiple (five) watermarkings	0.017	0.010	0.011	0.010

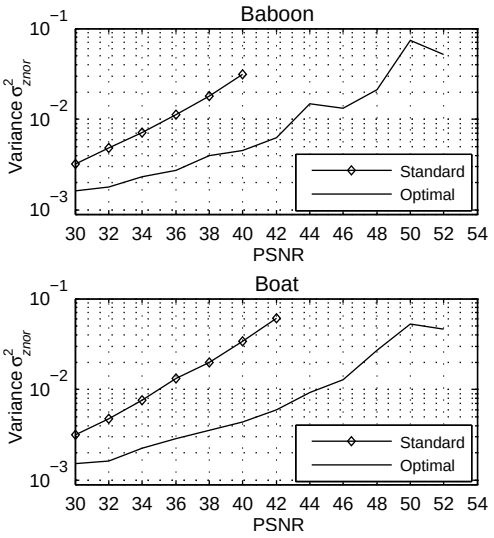

Figure 3: The σ^2_{znor} versus PSNR curves. Only the σ^2_{znor} values for the successful detection are shown.

very low watermark will be validated. To this end, we calculated σ^2_{znor} for the PSNR that changes from 30dB to 54dB in increments of 2dB. The corresponding curves are shown in Figure 3. With this setup, the highest PSNR value for which the standard detector detects the embedded watermark is 40dB ($\overline{\alpha} = 0.1323$) for Baboon and 42dB ($\overline{\alpha} = 0.0736$) for Boat, whereas the optimal one still detects the watermark for PSNR $= 52$dB ($\overline{\alpha} = 0.0331$) for Baboon and 52dB ($\overline{\alpha} = 0.0234$) for Boat.

5. CONCLUSION

In this paper, the problem of detection optimization for the DCT-domain image watermarking system is investigated. We optimized detection by modifying the searched watermark in order to maximize the correlation between the searched watermark and watermarked DCT coefficients. In addition to the improvement over the standard detection for both non-attacked and attacked images, the optimal detector allows detection of much weaker watermarks. The additional requirement of the optimization are the DCT coefficients the watermark is embedded into.

6. ACKNOWLEDGEMENT

This work is supported in part by the Ministry of Education and Science of Montenegro.

REFERENCES

[1] I. J. Cox, J. Kilian, F.T. Leighton, and T. Shamoon, "Secure spread spectrum watermarking for multimedia," *IEEE Trans. Image Process.*, vol. 6, pp. 1673-1687, Dec. 1997.

[2] P. Bassia, I. Pitas, and A. Nikolaidis, "Robust audio watermarking in time-domain", *IEEE Trans. Multimedia*, vol. 3, pp. 232-241, June 2001.

[3] W.-N. Lie and L.-C. Chang, "Robust and high-quality time-domain audio watermarking based on low-frequency amplitude modification", *IEEE Trans. Multimedia*, vol. 8, pp. 46-59, Feb. 2006.

[4] A. Bors and I. Pitas, "Image watermarking using *DCT* domain constrain", *IEEE Proc. of ICIP*'96, vol. 3, Lausanne, Switzerland, Sept. 1996, pp. 231-234.

[5] V. Solachidis and I. Pitas, "Circularly symmetric watermark embedding in 2-D DFT domain", *IEEE Trans. Image Process.*, vol. 10, pp. 1741-1753, Nov. 2001.

[6] S. Pereira, S. Voloshynovskiy, and T. Pun, "Effective channel coding for DCT watermarks", in *Proc. of IEEE ICIP*, 2000, vol. 3, pp. 671-673.

[7] M. Barni, F. Bartolini, V. Capellini, and A. Piva, "A DCT-domain system for robust image watermarking," *Signal Processing*, vol. 66, pp. 357-372, May 1998.

[8] S. Stanković, I. Djurović, and I. Pitas, "Watermarking in the space/spatial-frequency domain using two-dimensional Radon-Wigner distribution, *IEEE Trans. Image Process.*, vol. 10, pp. 650-658, Apr. 2001.

[9] A. Giakoumaki, S. Pavlopoulos, and D. Koutsouris, "Multiple digital watermarking applied to medical imaging", in *Proc. of IEEE Int. Conf. on EMS*, 2005, pp. 3444-3447.

[10] C. D. Meyer, *Matrix analysis and applied linear algebra*, SIAM, Philadelphia, USA, 2000, pp. 549-550.